NASA/TM—1998-208486

AIAA–98–3112

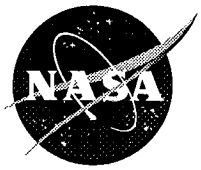

Model Engine Performance Measurement From Force Balance Instrumentation

Robert J. Jeracki
Lewis Research Center, Cleveland, Ohio

Prepared for the
34th Joint Propulsion Conference
cosponsored by AIAA, ASME, SAE, and ASEE
Cleveland, Ohio, July 12–15, 1998

National Aeronautics and
Space Administration

Lewis Research Center

July 1998

Available from

NASA Center for Aerospace Information
7121 Standard Drive
Hanover, MD 21076
Price Code: A03

National Technical Information Service
5287 Port Royal Road
Springfield, VA 22100
Price Code: A03

AIAA–98–3112

MODEL ENGINE PERFORMANCE MEASUREMENT FROM FORCE BALANCE INSTRUMENTATION

Robert J. Jeracki
NASA Lewis Research Center
Cleveland, Ohio

Abstract

A large scale model representative of a low-noise, high bypass ratio turbofan engine was tested for acoustics and performance in the NASA Lewis 9- by 15-Foot Low-Speed Wind Tunnel. This test was part of NASA's continuing Advanced Subsonic Technology Noise Reduction Program. The low tip speed fan, nacelle, and an un-powered core passage (with core inlet guide vanes) were simulated. The fan blades and hub are mounted on a rotating thrust and torque balance. The nacelle, bypass duct stators, and core passage are attached to a six component force balance. The two balance forces, when corrected for internal pressure tares, measure the total thrust-minus-drag of the engine simulator. Corrected for scaling and other effects, it is basically the same force that the engine supports would feel, operating at similar conditions. A control volume is shown and discussed, identifying the various force components of the engine simulator thrust and definitions of net thrust. Several wind tunnel runs with nearly the same hardware installed are compared, to identify the repeatability of the measured thrust-minus-drag. Other wind tunnel runs, with hardware changes that affected fan performance, are compared to the baseline configuration, and the thrust and torque effects are shown. Finally, a thrust comparison between the force balance and nozzle gross thrust methods is shown, and both yield very similar results.

Symbols

A	Area, ft^2
C_D	Nozzle exit discharge coefficient, W/W_{Ideal}
C_V	Nozzle exit velocity or thrust coefficient, V/V_{Ideal}
F	Force, lbf
F_G	Gross thrust, lbf
F_N	Standard net thrust (between station 0 and nozzle exits), lbf
F_N'	Basic overall net thrust ($W_\infty * V_\infty - W_0 * V_0$), lbf
F_{N^*}	Modified net thrust (defined to exclude the ϕ_{post} streamline integral), lbf
FNB_C	Bypass flow net thrust (station 0 to 19) corrected to standard day conditions, lbf
FNC_C	Core flow net thrust (station 0 to 9) corrected to standard day conditions, lbf
FNT_C	Total flow net thrust (station 0 to 9 & 19) corrected to standard day conditions, lbf
p	Static pressure, psi

Symbols (cont.)

PT	Total pressure, psi
RPMc	Rotor rpm corrected to standard day conditions, rpm
RPMck	RPMc/1000, rpm/1000
SHPc	Shaft horsepower, corrected to standard day conditions, hp
Tares	Force correction from internal (pressure-p_0)*area terms, lbf
TH1c	Thrust on the rotor balance minus Tares, corrected to standard day conditions, lbf
TH2c	Thrust on the cowl balance minus Tares, corrected to standard day conditions, lbf
THCBc	Raw force read by the cowl balance, corrected to standard day conditions, lbf
THRBc	Raw force read by the rotor balance, corrected to standard day conditions, lbf
THTc	Total thrust minus Tares, corrected to standard day conditions, lbf
TQRBc	Torque read by the rotor balance, corrected to standard day conditions, ft-lbf
V	Velocity, ft/sec
W	weight flow, slug/sec
Greek	
γ	Specific heat ratio of air (1.4)
ϕ	Surface pressure and friction force, lbf
τ	Surface friction force, lbf
Subscripts	
AB	Afterbody
Afterbodies	Fan and core afterbodies
Cowl	Cowl, stator, and aft duct flowpath
FB	Total of force balances and internal pressure tares
Ideal	Calculated with average nozzle conditions and physical nozzle area
INT	Internal, behind rotor, and fore and aft of cowl balance
Nacelle	Nacelle from inlet highlight to bypass nozzle exit
Nozzles	Both bypass and core nozzles
pre	pressure*area integral on flow streamtube upstream of inlet
post	pressure*area integral on flow streamtube downstream of bypass nozzle
Rotor	Rotor blades and hub
0	Freestream far upstream
1	Inlet highlight station
9	Core nozzle exit station
19	Bypass nozzle exit station
∞	Freestream far downstream

Introduction

Fan engine performance methods have been developed, refined, and standardized through years of experience. Methods include component tests (inlet, fan, stage, and nozzle), ground test, and Altitude Test Facilities (ATF). Flow-through nacelles and small Turbine Powered Simulators (TPS) have normally been used to evaluate installation effects. Larger TPS models with strain gaged force balances may be used to measure fan engine performance in wind tunnels.

SAE Technical Committee E-33, "In-Flight Propulsion Measurement", has reported on standard methods of thrust determination beginning with Aerospace Information Report (AIR) 1703, "In-Flight Thrust Determination" (Ref. 1). That report on steady-state thrust and uncertainty is currently being updated. Separately, a new report is being written which deals with the special problems associated with thrust measurement of very high bypass ratio and low fan pressure ratio Advanced Ducted Propulsor (ADP) or other Ultra-High Bypass (UHB) fan engines. With several US engine companies, NASA Lewis is continuing to test 22-inch diameter fan models of existing and advanced engines to evaluate low noise improvement possibilities. This is part of NASA's Advanced Subsonic Technology Noise Reduction Program.

A 22-inch fan diameter model simulating a low tip speed, ADP type engine is shown in the NASA Lewis 9- by 15-Foot Low-Speed Wind Tunnel (Fig. 1 photo). The simulator is mounted forward of a high-pressure air turbine, which is on top of a support strut and turntable. The strut carries heated air to the turbine, lubrication lines to and from the model, and instrumentation leads off of the model to the high-speed data system. A cross section of the simulator is shown in Figure 2. The engine core is simulated by an inlet, inlet guide vanes, a flow-through duct with support struts, and a nozzle. The nozzle area was expanded to pass the correct core flow, so it does not represent the exact geometry of the engine being simulated. If the core is modeled with a first compressor stage, the nozzle simulation can match the engine.

Force Components and Net Thrust Definitions

The fan blades and hub are mounted on a rotating thrust and torque balance. The nacelle, bypass duct stators, and core passage are attached to a six component force balance. The two balance forces, when corrected for internal pressure tares, measure the total thrust-minus-drag of the engine simulator. Corrected for scaling and other effects, it is basically the same force that the engine supports would feel, operating at similar conditions. Figure 3 shows a control volume that identifies the various force components of the engine simulator thrust. The tare-corrected balance force (F_{FB} - Tares = $F_{Rotor} + F_{Cowl} - \Sigma\,(p_{INT}-p_0)*A_{INT}$) is equal to all other forces on the fan and nacelle including:

the change in the gross thrust from the inlet to the nozzle exits,

$$F_{G19} + F_9 - F_{G1} = W_{19}*V_{19} + (p_{19}-p_0)*A_{19} + W_9*V_9 + (p_9-p_0)*A_9 - W_1*V_1 + (p_1-p_0)*A_1 \qquad (1)$$

fan and core afterbody pressure and friction (τ) forces,

$$\phi_{Fan\ AB} = \int_{Fan\ AB} (p-p_0)*dA + \tau \quad \text{and} \quad \phi_{Core\ AB} = \int_{Core\ AB} (p-p_0)*dA + \tau \qquad (2)$$

and external nacelle pressure and friction force

$$\phi_{Nacelle} = \int_{Nacelle} (p-p_0)*dA + \tau \quad (3)$$

The definitions of net thrust that follow are consistent with SAE AIR 1703 (Ref. 1) which also references the definitions in AGARD report AG-237 (Ref. 2). The basic overall net thrust is defined as the net change in momentum from far upstream to far downstream of the engine ($F_N' = W_\infty*V_\infty - W_0*V_0$). That definition includes the thrust the engine provides to the mass flow and the pressure-times-area integral on the flow streamtube upstream of the inlet (ϕ_{pre}, pre-entry force or additive drag), and an equivalent integral on the jet streamtube downstream of the nozzle (ϕ_{post}, post exit force). The control volume shown includes the equivalent nozzle exit and afterbody components, not the post exit force as a component. The force balance, however, senses only the forces exerted on the fan/nacelle hardware and not those streamtube forces.

The force balance measurement and force component summations to get net thrust are shown in the following equations:

$$F_{FB} - Tares = F_{G,\,Nozzles} - F_{G1} + (\int_{Afterbodies} (p-p_0)*dA + \tau) + (\int_{Nacelle} (p-p_0)*dA + \tau) \quad (4)$$

Where, τ is the friction force on the surface. Substituting ($W_0*V_0 - \phi_{pre}$) for F_{G1}

$$\begin{aligned} F_{FB} - Tares = {} & W_{19}*V_{19} + (p_{19}-p_0)*A_{19} + W_9*V_9 + (p_9-p_0)*A_9 - W_0*V_0 \\ & + (\int_{Fan\ AB} (p-p_0)*dA + \tau) + (\int_{Core\ AB} (p-p_0)*dA + \tau) - \phi_{pre} \\ & + (\int_{Nacelle} (p-p_0)*dA + \tau) \end{aligned} \quad (5)$$

The terms in the first line are the standard net thrust, F_N, (or just net thrust). Including the afterbody pressure integrals (from the second line) gives the modified standard net thrust, F_N^*. Where, F_N^* is defined to exclude the ϕ_{post} term in the definition of net thrust and account for it as a drag term. The calculation of modified standard net thrust from the simulator force balances requires the following:

$$F_N^* = (F_{FB} - Tares) + \phi_{pre} - (\int_{Nacelle} (p-p_0)*dA + \tau) \quad (6)$$

Since, for subsonic testing ϕ_{pre} (-additive drag) is basically zero, then

$$F_N^* \cong (F_{FB} - Tares) - (\int_{Nacelle} (p-p_0)*dA + \tau) \quad (7)$$

If ϕ_{post} is added back into the equation, the result is the defined overall net thrust, F_N'.

$$F_N' = (F_{FB} - Tares) + (\phi_{pre} + \phi_{post}) - (\int_{Nacelle} (p-p_0)*dA + \tau) \quad (8)$$

In a control volume from the flow streamlines and nacelle out to infinity, the sum ($\phi_{pre} + \phi_{post}$) should be very nearly zero (the overall change in momentum representing the nacelle external drag), unless the external flow is disturbed by shocks, flow separations, etc.

$$F_N' \cong (F_{FB} - \text{Tares}) - (\int_{Nacelle} (p-p_0)*dA + \tau) \quad (9)$$

So, the measured force most closely represents the overall net thrust, when corrected for the external nacelle drag.

Typical engine test stands and altitude test facilities are designed to measure engine gross thrust. With isolated inlet and nozzle tests for losses and external drag, the results are correlated and thrust is calculated using nozzle flow or discharge coefficient (C_D) and velocity coefficient (C_V). Engine net thrust can then be calculated from the gross thrust by subtracting the ram drag (W_0*V_0) and calculated nacelle drag. Industry has developed the tools to calculate thrust very accurately using nozzle gross thrust, and is the industry standard method of thrust measurement. As an option, a large simulator measures the scaled engine model total thrust-minus-drag directly. The nacelle drag is included in the measurement and duct total pressure and temperature measurements are not needed for thrust evaluation. They are used, however, to generate pressure and efficiency maps for the scale model fan as would be done for an engine in a test facility. The difficulty with ϕ_{pre} and ϕ_{post}, discussed above for simulator testing, only arises when net and gross thrust are needed, instead of the direct thrust-minus-drag as measured.

Force Balance Corrections

Several corrections or adjustments were made to the raw force balance signals to improve accuracy. The excitation voltage applied to the balances, for each primary balance component, was measured at the balance, along with the balance signals. Any difference between the measured excitation voltage and the calibration reference was used to adjust the balance signal. This was especially important for the rotor balance. The long thin wires leading through the shaft to the slip ring added resistance that changed as the temperature increased while powering the fan. The actual applied excitation voltage was reduced, but using the voltage measurement corrected the problem.

Room temperature calibrations were the source of the primary and interaction coefficients (converting from millivolts to forces) for the balances. High temperature calibrations also were done and allowed the slight effects on balance gain to be corrected at elevated balance temperature. Balance temperature change also created a zero-shift in the balance signals. Post-run zeros were used to determine the balance signal zero-shift versus temperature. Applying this temperature-based correction reduced the post-run zero shifts significantly. The final "hot balance" post-run zeros were used as new reference points for powered, "hot" test data points.

Force Balance Results

Among the 62 tunnel runs that were made during this test entry, several were acoustic configurations with nearly identical fan/nacelle test hardware. Runs 42, 43, and 48-55 are acoustically "clean" runs with no rakes or other disturbances. They differ in acoustic liners installed in the inlet, between the fan and stator, and/or in the nozzle, except for Vortex Generators (VGs) installed on the fan blade trailing edges in Runs 48 and 49. The tunnel freestream Mach number was set to 0.10. These runs should have the same performance, and have been used to investigate the force balance repeatability. The corrected rotor balance torque and shaft horsepower (corrected to standard day conditions, TQRBc and SHPc) are shown in Figures 4 and 5, versus corrected RPM/1000 (RPMck). There are no large differences between runs, except that Runs 48 and 49 have slightly lower torque and power. Those are the runs with the fan blade VGs installed. At several RPMck values many repeated acoustic data points were recorded, resulting in overlapping of the data symbols. The corrected rotor torque is the most accurate and repeatable of the balance force measurements. The corrected rotor balance force (THRBc) is shown two ways in Figures 6 and 7. Figure 6 uses corrected RPM/1000 as the X-axis, and Figure 7 uses the corrected rotor torque. Slightly larger differences between runs can be seen for the rotor balance force than for the rotor torque. The differences that showed up in rotor torque with the fan VGs are not obvious in the rotor thrust. The rotor balance force variation with torque (Fig. 7) is nearly a straight line.

The rotor balance force includes pressure forces on the aft face of the rotor hub, which are not part of the desired model flow path thrust. The rotor thrust (including hub external force) is calculated by adjusting the rotor balance force for these internal pressure tare forces ($TH1 = F_{Rotor} - (p_{Rotor} - p_0)*A_{Rotor}$). The rotor corrected thrust (TH1c) is shown in Figures 8 and 9, with the same X-axes as the rotor balance force figures. The rotor thrust values are higher than the rotor balance force values due to the pressure tare force adjustment, but the tare adjustment had no effect on the run-to-run differences.

The cowl balance corrected force (THCBc) is shown in Figures 10 and 11, with the same X-axes as before. Run 43 shows erratic cowl balance force variation below 8,000 RPMc. It was confirmed that this is in the balance signal. This run will be eliminated from later plots. Somewhat larger differences between runs can be seen for the cowl balance force than for the rotor balance force. The cowl balance force variation with rotor torque is nearly a straight line, as the rotor force was.

Like the rotor thrust, the cowl thrust (thrust-minus-drag) is calculated by adjusting the cowl balance force for internal pressure tare forces. The cowl corrected thrust (TH2c) is shown in Figures 12 and 13, with the same X-axes as before. The cowl thrust values are lower than the cowl balance force value (tare effect), but the tare adjustment had no effect on the run-to-run differences.

The total thrust-minus-drag of the engine model is calculated by adding the rotor and cowl thrusts. The total corrected thrust (THTc) is shown in Figures 14 and 15. The run-to-run differences are comparable to the cowl balance results. In this case the internal pressure

tare forces are reduced because a large portion of the tare acts in one direction on the aft rotor face and in the opposite direction on the cowl balance forward face.

Thrust Balance Comparison With Treated Rubstrip

Part of the wind tunnel testing was done with a treated fan rubstrip, to increase fan stall margin. Two acoustic runs were made with the treated rubstrip installed. In addition to the acoustic comparison, the force balances were used to evaluate the effect the rubstrip has on thrust and torque. The total corrected thrust (THTc) is shown in Figure 16, versus RPMc/1000. The smooth rubstrip data (all data that was previously shown but eliminating Run 43) are shown and compared to the two runs with the treated rubstrip installed. As noted above, the smearing of data at certain RPMck values is the result of scatter between many repeated acoustic data points that were recorded. This scatter will be discussed later in the report. For the treated rubstrip design, there is a noticeable penalty in total thrust. Figure 17 shows the corrected rotor torque (TQRBc), which is also lower with the treated rubstrip installed. Since both thrust and torque were reduced, a comparison of the total corrected thrust variation with corrected rotor torque is shown in Figure 18. There is only a little difference between the smooth and treated rubstrips. A large effect of the treated rubstrip seems to have been to move the fan to different points on a thrust-versus-torque operating line. The force balances clearly showed the change.

Thrust Calculated from Nozzle Coefficients

In the previous discussions of net thrust measurement, the use of duct pressure and temperature rakes to map fan performance was mentioned briefly. Mapping fan and stage pressure ratio and flow on the actual fixed-nozzle operating line gives a capability to calculate nozzle flow conditions and the gross and net thrust of the simulator, when the rakes are removed for acoustic testing. Fan pressure ratio and weight flow measurements correlated well with corrected speed (RPMc), so, curve fits were made available for the acoustic run data analysis. The treated rubstrip resulted in different pressure ratio and flow curves versus RPMc.

Only one measurement (at takeoff fan speed) was made of stator pressure loss in the bypass duct, however. That loss and a nozzle pressure loss are needed to have accurate nozzle "exit" conditions, and result in a good calculation of nozzle gross thrust. The single survey of stator pressure loss, and an approximation of the loss variation with duct flow rate were used to calculate the nozzle exit total pressure. A curve fit of nozzle velocity coefficient, C_V, from a similar nozzle and a constant discharge coefficient, C_D, were used as the estimated nozzle coefficients. Normally these coefficients would be measured in a nozzle test facility. The bypass flow net thrust was calculated from the gross thrust and ram drag as:

$$FNB = 7*((PT_{19}/P_0)^{(\gamma-1)/\gamma} - 1) * C_{V,19} * C_{D,19} * P_0 * A_{19} - W_{19} * V_0 \quad (10)$$

The core nozzle design was nearly a cylinder, with pressure and temperature rakes installed just before the nozzle. Little loss would be expected, so high core nozzle C_V and C_D coefficients were estimated and used for calculating core gross thrust. The core flow net thrust was calculated from the gross thrust and ram drag as:

$$FNC = 7*((PT_9/P_0)^{(\gamma-1)/\gamma} - 1) * C_{V,9} * C_{D,9} * P_0 * A_{19} - W_9 * V_0 \quad (11)$$

The total net thrust was calculated as the sum of the bypass and core net thrusts.

The freestream Mach number was 0.10 for the acoustic runs. As a result, the nacelle external drag was estimated to be small (less than 5 lbf, compared to total thrust scatter of about ±10 lbf). No attempt has been made to include this small drag adjustment to the summary results shown in the figures showing net thrust.

The gross and net thrust calculations were done for the acoustic wind tunnel runs compared above. The bypass, core, and total corrected net thrust values (from nozzle gross thrust calculations) are shown in Figures 19 to 21, versus RPMc/1000. The core net thrust (Fig. 20) is nearly zero, so bypass net thrust is almost total net thrust for this un-powered core simulation.

The total corrected net thrust (Fig. 21) shows very similar characteristics to the total corrected thrust from the balance forces (Fig. 16). Both thrust methods show the treated rubstrip with a thrust (operating line) reduction. A direct comparison of the total thrust-minus-drag from the balance forces and the total corrected net thrust is shown Figure 22. A perfect agreement would be all data points falling along a diagonal line from zero to 1600 lbf. The agreement is actually quite good. Most points appear shifted in the lower net thrust direction, some of which should be the effect of the external nacelle drag. Where there are many repeated data points (e.g. about 1250 lbf) the total corrected thrust (Y-axis) shows a drift or scatter. This appears to be the limit of the force balance repeatability, with run-to-run and thermal variations, and will be discussed in the next section. The net thrust does not scatter much because it is mostly based on the pressure ratio and flow curve fits.

Performance and Repeatability Near Takeoff

The previous figures show the force balance values for thrust to be reasonably accurate and repeatable. The plot scales are large, and do not allow evaluation of the error band of the measurements. Figures 23 to 29 show the details of the force balance measurements, using expanded scales centered around the takeoff operating point (8,750 RPMc). The bypass net thrust equation can be used with the nozzle conditions near takeoff, to get a sense of the accuracy needed to measure small changes in duct pressure loss. If a 0.10 percent error or change in nozzle total pressure is assumed (about 0.0185 psi), slightly over 6.4 lbf change in bypass net thrust results (0.52 percent change in net thrust). If the weight flow is known accurately, the change in net thrust is reduced to 3.1 lbf (0.26 percent change).

Rotor balance corrected torque is shown in Figure 23. For each of the three test configurations shown, the variation between runs is about ±4 ft-lbf. That is ±0.66 percent of the average torque (about 610 ft-lbf), and ±0.26 percent of the 1,530 ft-lbf full scale torque for the rotating balance. The overall torque accuracy from the balance calibration at room temperature was ±0.25 percent of full scale. The few points of smooth rubstrip data with fan blade VGs on the fan blades can be seen at about 10 ft-lbf (1.64 percent) below the baseline, smooth rubstrip data. The treated rubstrip torque is about 20 ft-lbf (3.28 percent) below the baseline smooth rubstrip.

Rotor balance corrected thrust is shown in Figures 24 and 25. Figure 25 used the rotor balance corrected torque as the X-axis to show any effect an operating line change might have on the indicated scatter. For the test configurations shown, the variation between runs is about ±6 lbf. That is ±0.67 percent of the average thrust (about 900 lbf), and ±0.30 percent of the 2,000 lbf full scale thrust for the rotating balance. The overall thrust accuracy from the balance calibration at room temperature was ±0.23 percent of full scale. The smooth rubstrip with fan VGs on the fan blades is only 4 lbf below the smooth rubstrip configuration. That shows up best on Figure 25 because the torque (X-axis) changed enough to make the data points stand out. The treated rubstrip thrust is about 40 lbf below the baseline smooth rubstrip data. However, Figure 25 shows the source of most of the thrust loss is the lower operating torque. At about 640 ft-lbf torque, a second set of treated rubstrip data appears on this plot (a higher RPMc). Interpolating at the same torque level, the treated rubstrip rotor thrust is only about 15 ft-lbf below that of the smooth rubstrip. That would be the penalty if the fan speed were increased to compensate for the treated rubstrip.

Cowl balance corrected thrust is shown in Figures 26 and 27. As done for the rotor thrust, Figure 27 used the rotor balance corrected torque as the X-axis. For the test configurations shown, the variation between runs is about ±8 lbf. That is ±2.22 percent of the average thrust (about 360 lbf), and ±0.40 percent of the 2,000 lbf full scale thrust for the cowl balance. The overall thrust accuracy from the balance calibration at room temperature was ±0.10 percent of full scale. The fan VG thrust data is about 10 lbf lower than the baseline smooth rubstrip data. That shows up best on Figure 27, again because of the torque change. Surprisingly, the treated rubstrip thrust is about the same level as that of the baseline smooth rubstrip. Figure 27 shows there is some thrust loss from the lower operating torque, but some data points with the treated rubstrip jumped up about 10 lbf.

Total corrected thrust is shown in Figures 28 and 29. As done for the individual thrusts, Figure 29 used the rotor balance corrected torque as the X-axis. For the three configurations, the variation between runs is about ±10 lbf. That is ±0.78 percent of the average total thrust (about 1,290 lbf for the baseline), and ±0.25 percent of the total 4,000 lbf full scale thrust for the balances. The fan VG data is about 20 lbf (1.55 percent) lower than the baseline. The treated rubstrip thrust is about the 50 lbf (3.89 percent) lower than that of the baseline smooth rubstrip. Figure 29 shows most of that thrust loss is from the lower operating torque.

At the beginning of this section, the change in net thrust due to a 0.10 percent change in nozzle total pressure (a very accurate average measurement to make) was calculated to be 0.26 percent, if the weight flow is known accurately, The scatter or variations in average total thrust measured with the force balances are about three times that. So, about ±0.30 percent in nozzle pressure would be difficult to identify with the force balance measurements. The force balances were able to measure total thrust changes of 1.55 and 3.89 percent, and rotor torque changes of 1.64 and 3.28 percent, from the effects of fan blade VGs and treated rubstrip, respectively.

Summary of Results

A large scale model representative of a low-noise, high bypass ratio turbofan engine was tested for acoustics and performance in the NASA Lewis 9- by 15-Foot Low-Speed Wind Tunnel. The low tip speed fan, nacelle, and an un-powered core passage (with core inlet guide vanes) were simulated. The fan blades and hub are mounted on a rotating thrust and torque balance. The nacelle, bypass duct stators, and core passage are attached to a six component force balance. The two balance forces, when corrected for internal pressure tares, measure the total thrust-minus-drag of the engine simulator. Corrected for scaling and other effects, it is basically the same force that the engine supports would feel, operating at similar conditions. A control volume is shown and discussed, identifying the various force components of the engine simulator thrust and definitions of net thrust. Several wind tunnel runs with nearly the same hardware installed are compared, to identify the repeatability of the measured thrust-minus-drag. Analysis of run-to-run force balance scatter indicates torque repeatability is within ±0.66 percent of the torque near the takeoff operating point for this model. Measured repeatability of total thrust at takeoff was within ±0.78 percent of the takeoff total thrust. Other wind tunnel runs, with hardware changes that affected fan performance, are compared to the baseline configuration. The force balances were able to measure total thrust changes of 1.55 and 3.89 percent, and rotor torque changes of 1.64 and 3.28 percent, from the effects of fan blade vortex generators and treated rubstrip, respectively. A thrust comparison between the force balance and nozzle gross thrust methods is shown, and both thrust methods yielded very similar results.

References

1. Society of Automotive Engineers, "In-Flight Thrust Determination," SAE AIR 1703, Nov. 1985, Reaffirmed Dec. 1992.
2. MIDAP Study Group, "Guide to In-Flight Thrust Measurements of Turbojets and Fan Engines," AGARDOGRAPH AG-237, Jan. 1979.
3. Society of Automotive Engineers, "Gas Turbine Engine Performance Station Identification and Nomenclature," ARP 755A, Apr. 1974.

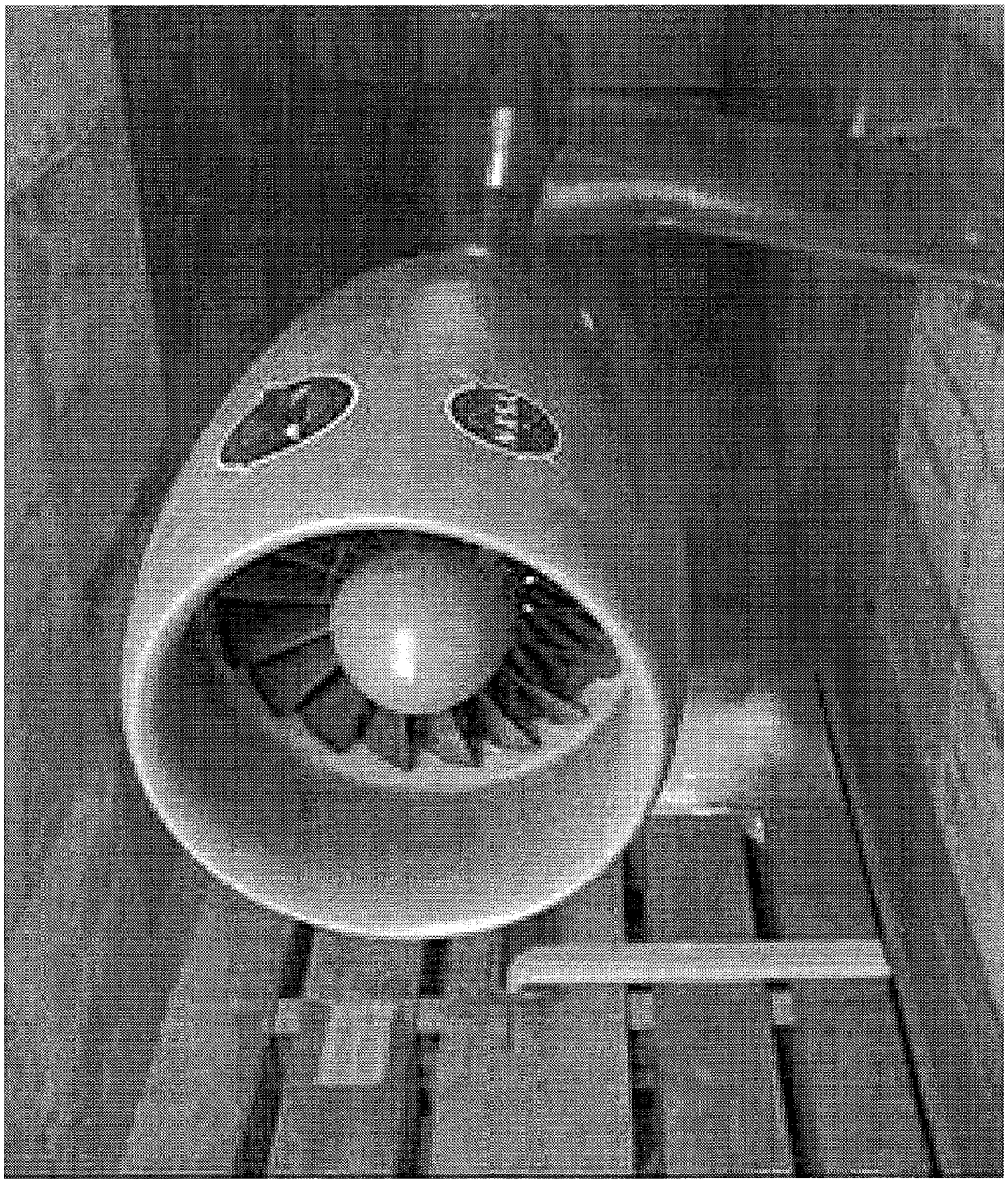

Figure 1. - ADP type engine model in the NASA Lewis 9- by 15-Foot Low-Speed Wind Tunnel.

Figure 2. - Cross section of an ADP model mounted on rotating and static strain gaged force balances.

NASA/P&W 22-Inch Fan/Nacelle Test Hardware

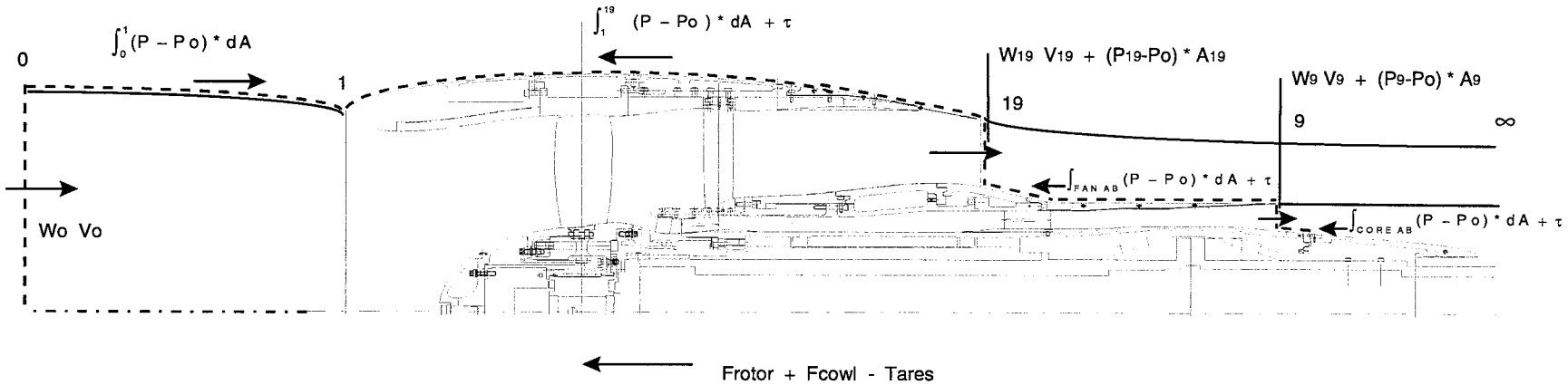

Figure 3. - Control volume that identifies the various force components in the engine simulator thrust.

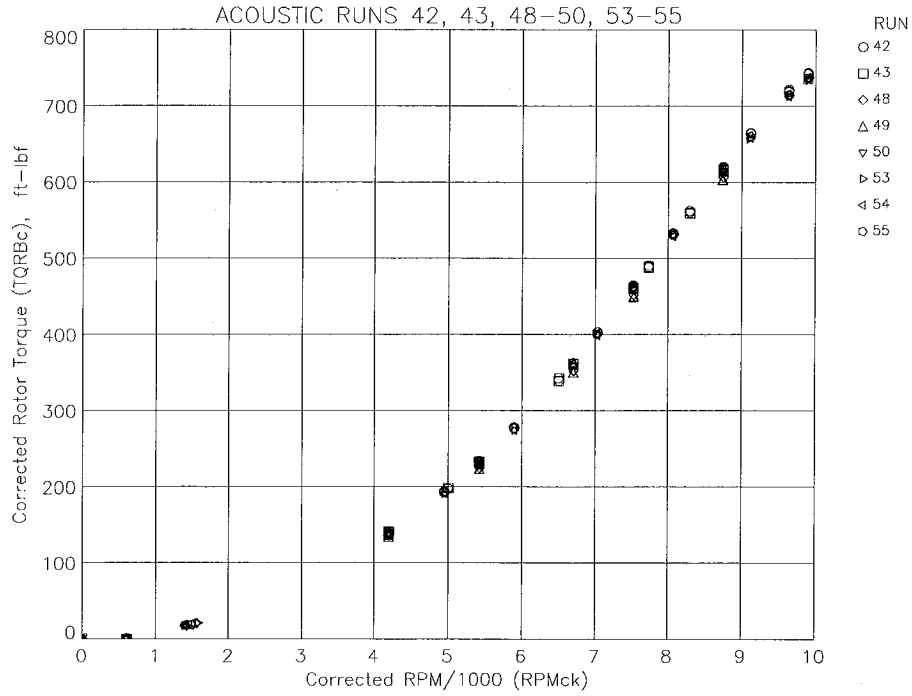

Figure 4. Rotor Balance Corrected Torque vs RPMc/1000, on Operating Line, Aeroacoustically Clean

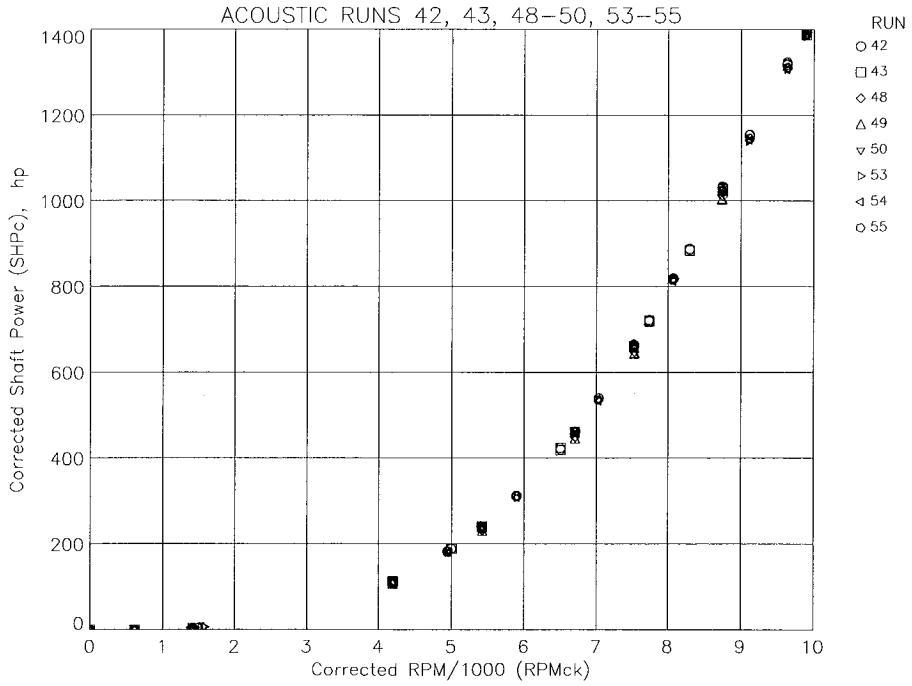

Figure 5. Rotor Balance Corrected Shaft Horsepower vs RPMc/1000, on Operating Line, Aeroacoustically Clean

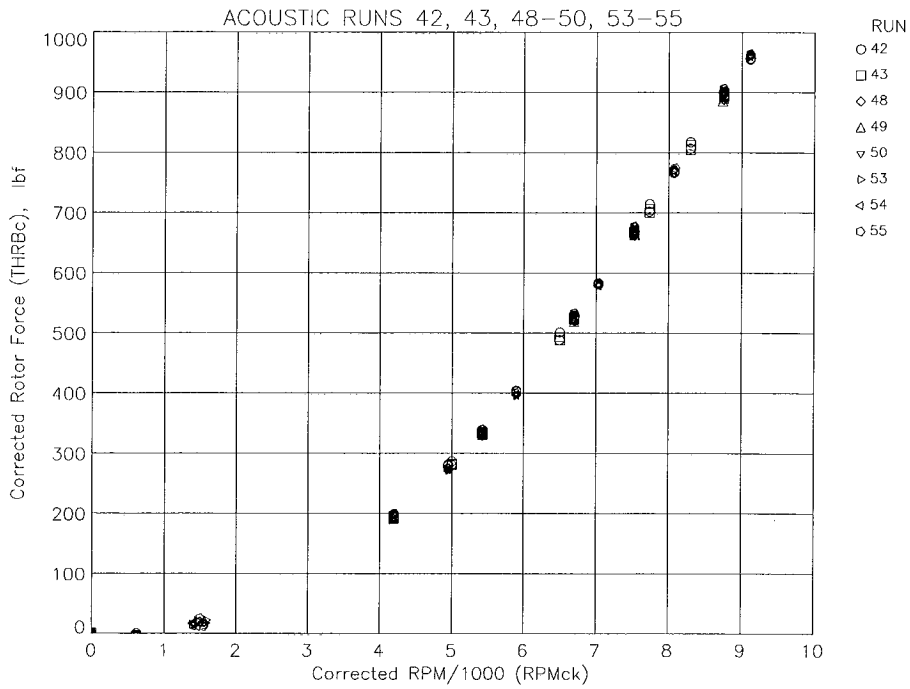

Figure 6. Rotor Balance Corrected Force vs RPMc/1000, on Operating Line, Aeroacoustically Clean

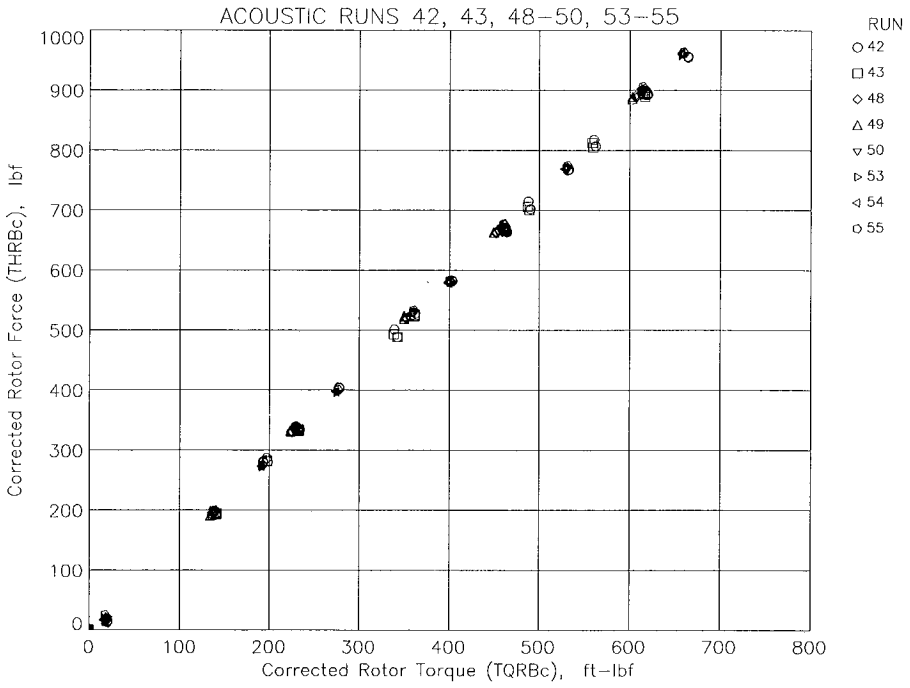

Figure 7. Rotor Balance Corrected Force vs Rotor Balance Corrected Torque, on Operating Line, Aeroacoustically Clean

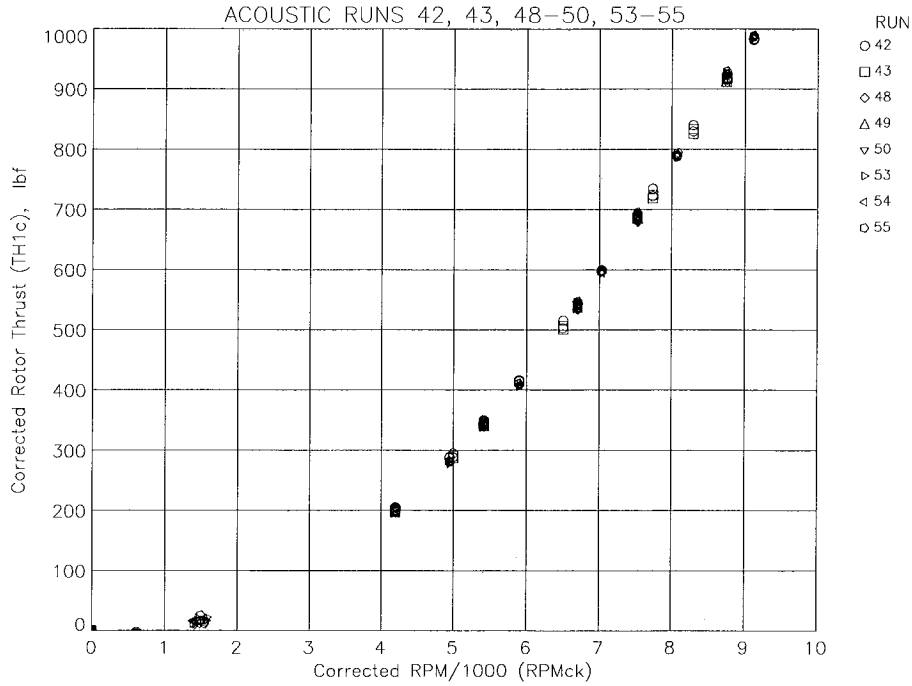

Figure 8. Rotor Balance Corrected Thrust vs RPMc/1000, on Operating Line, Aeroacoustically Clean

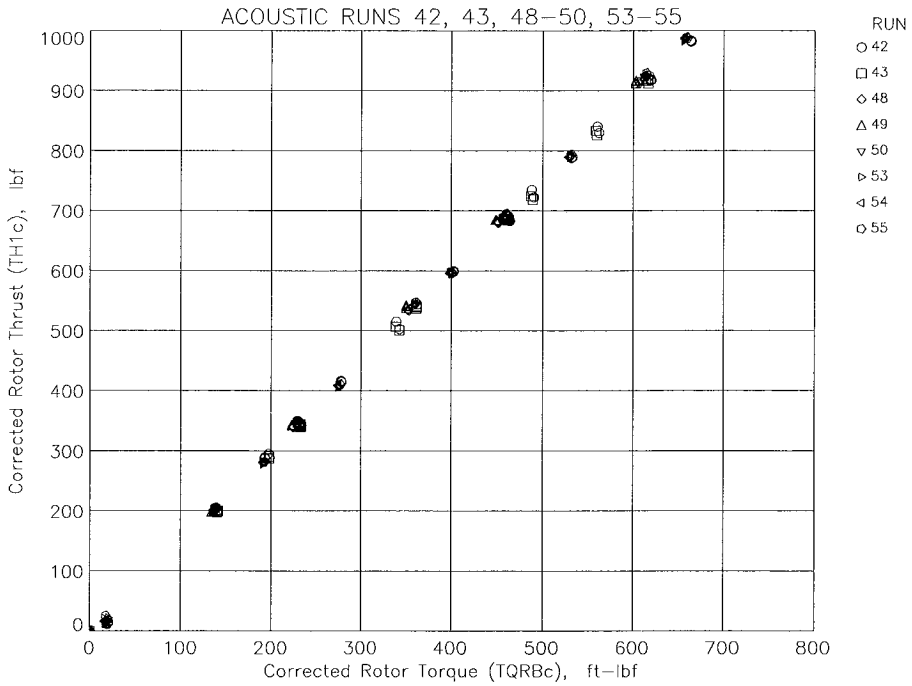

Figure 9. Rotor Balance Corrected Thrust vs Rotor Balance Corrected Torque, on Operating Line, Aeroacoustically Clean

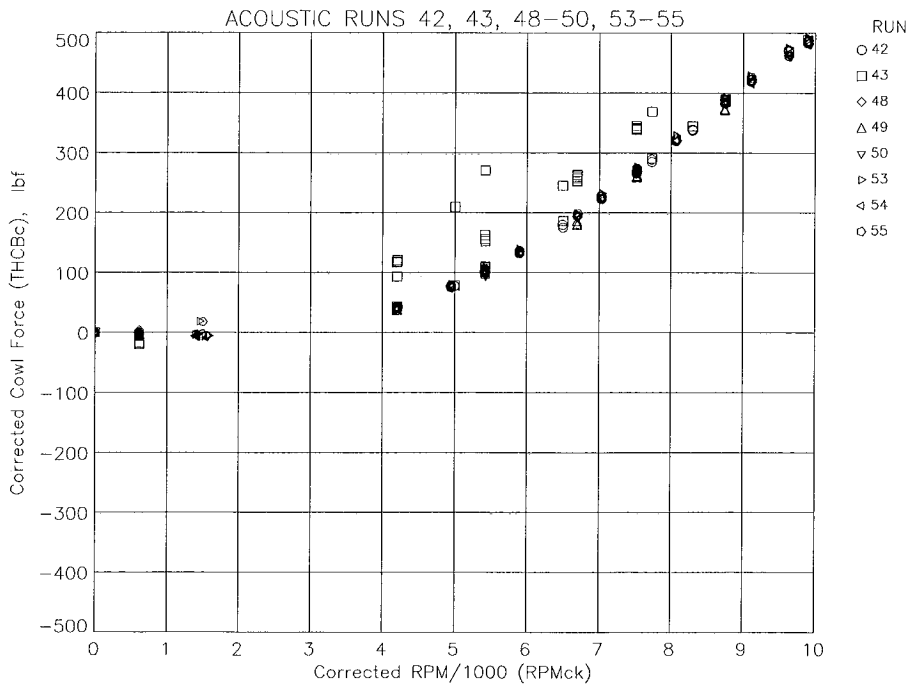

Figure 10. Cowl Balance Corrected Force vs RPMc/1000, on Operating Line, Aeroacoustically Clean

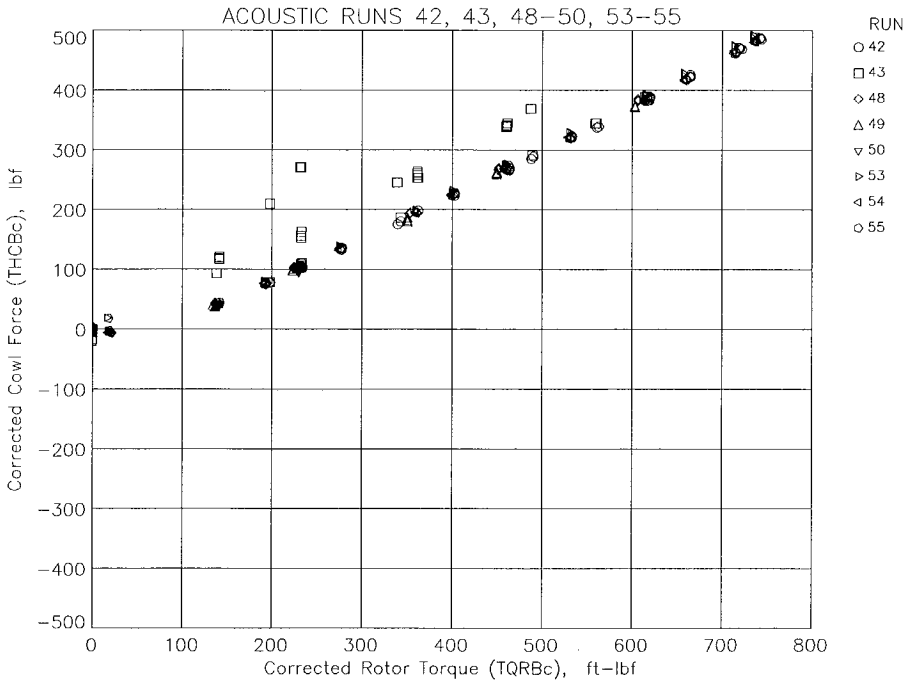

Figure 11. Cowl Balance Corrected Force vs Rotor Balance Corrected Torque, on Operating Line, Aeroacoustically Clean

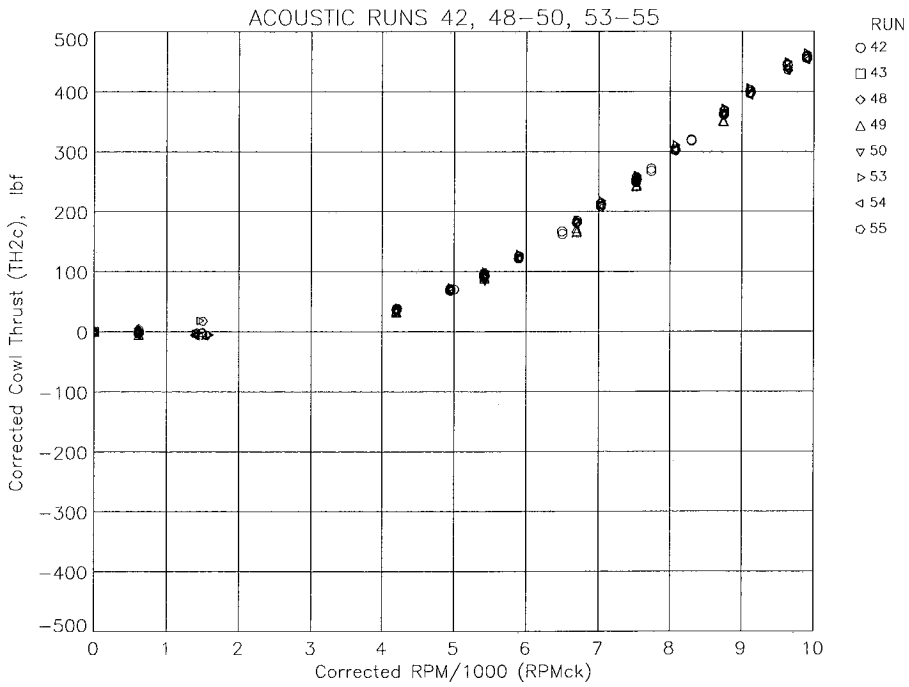

Figure 12. Cowl Balance Corrected Thrust vs RPMc/1000, on Operating Line, Aeroacoustically Clean

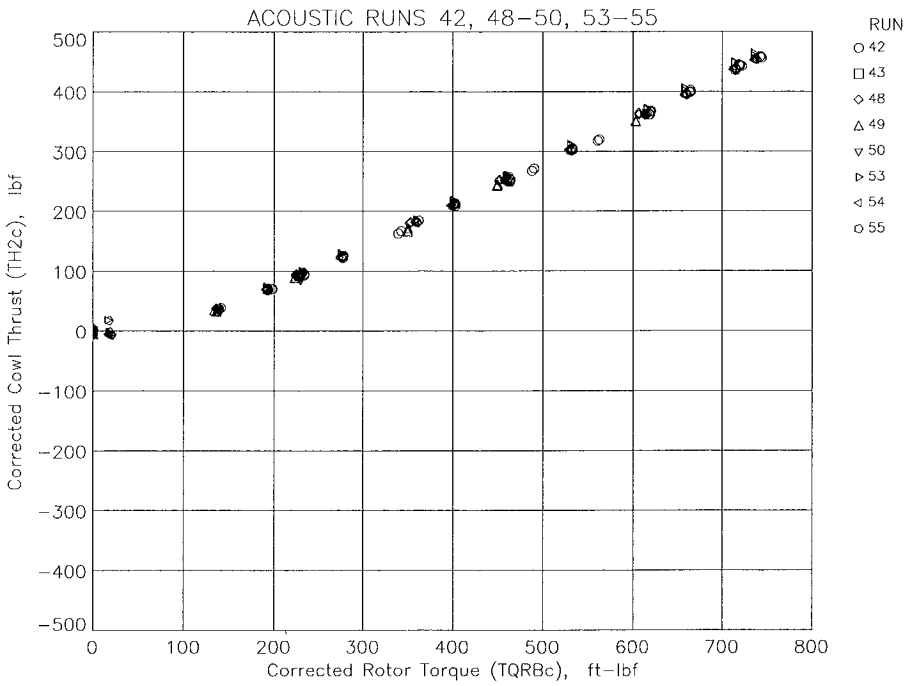

Figure 13. Cowl Balance Corrected Thrust vs Rotor Balance Corrected Torque, on Operating Line, Aeroacoustically Clean

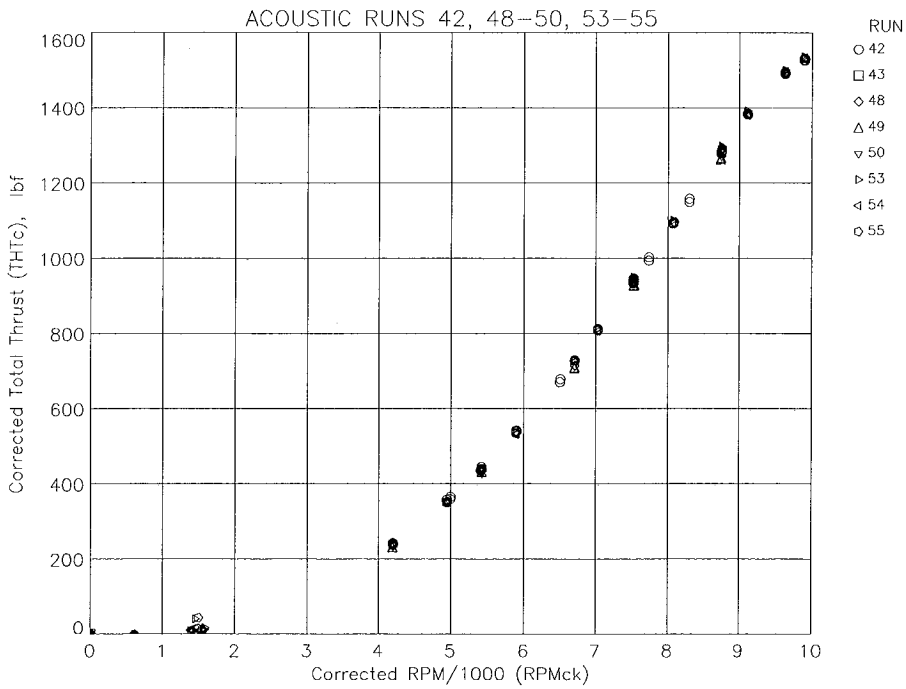

Figure 14. Total Corrected Thrust vs RPMc/1000, on Operating Line, Aeroacoustically Clean

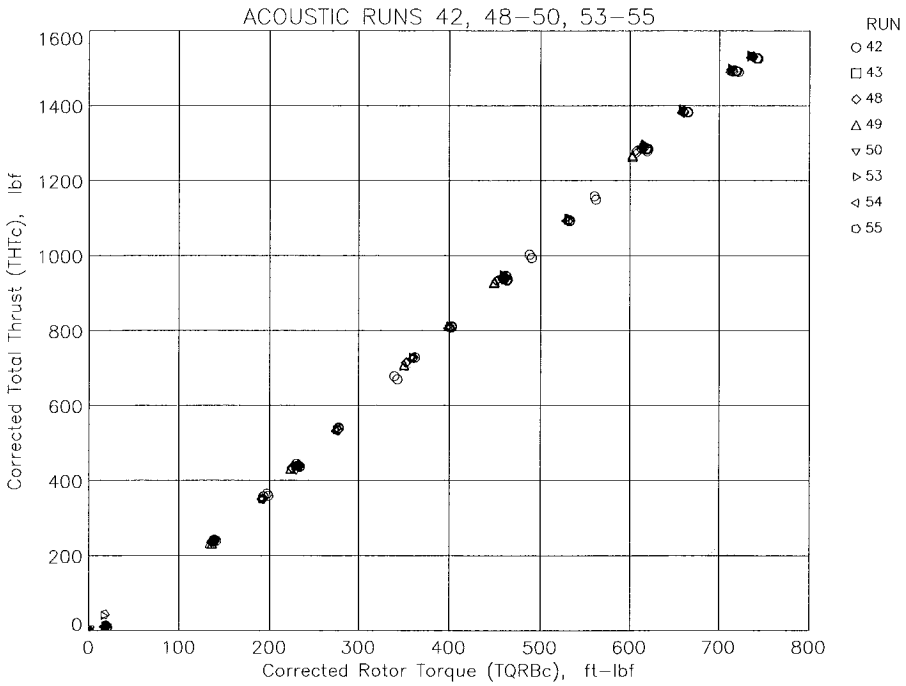

Figure 15. Total Corrected Thrust vs Rotor Balance Corrected Torque, on Operating Line, Aeroacoustically Clean

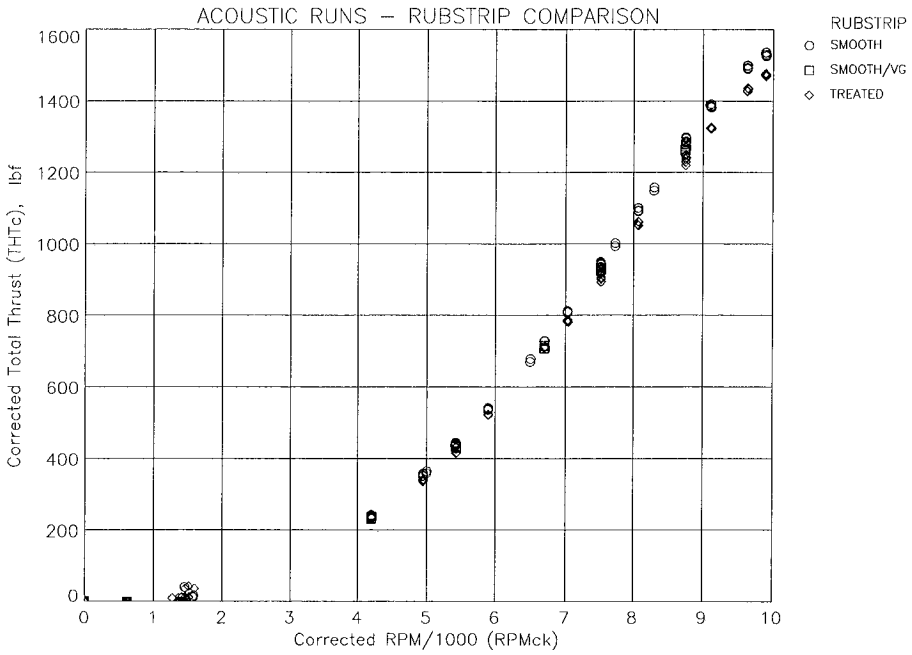

Figure 16. Total Corrected Thrust vs RPMc/1000, with Two Rubstrips, on Operating Line, Aeroacoustically Clean

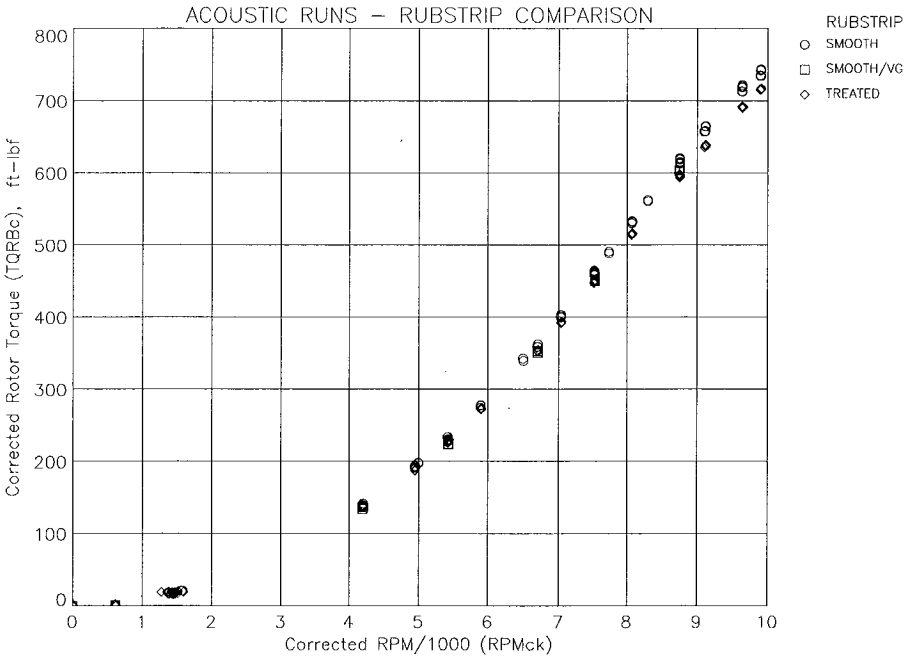

Figure 17. Rotor Balance Corrected Torque vs RPMc/1000, with Two Rubstrips, on Operating Line, Aeroacoustically Clean

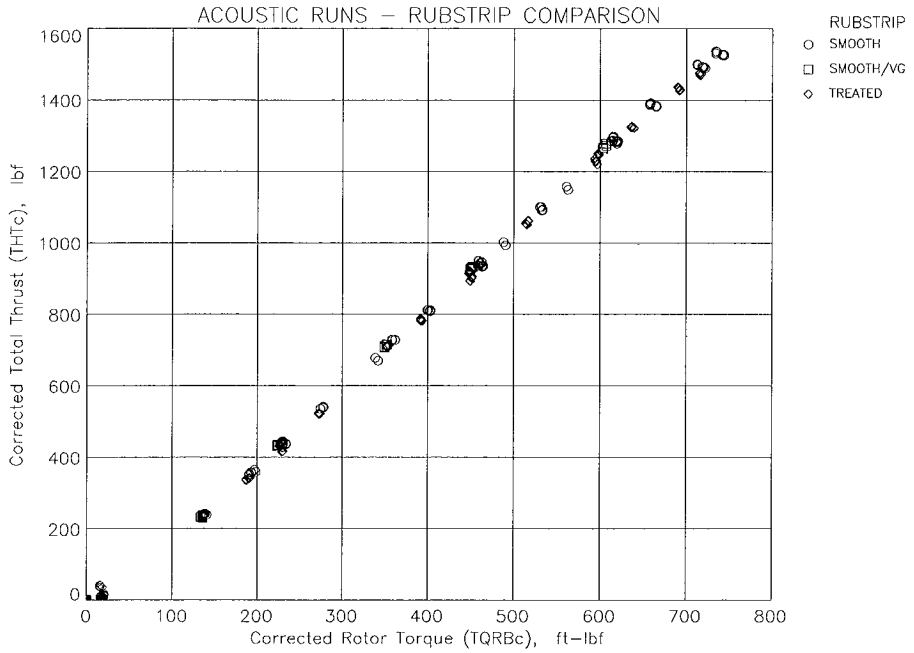

Figure 18. Total Corrected Thrust vs Rotor Balance Corrected Torque, with Two Rubstrips, on Operating Line, Aeroacoustically Clean

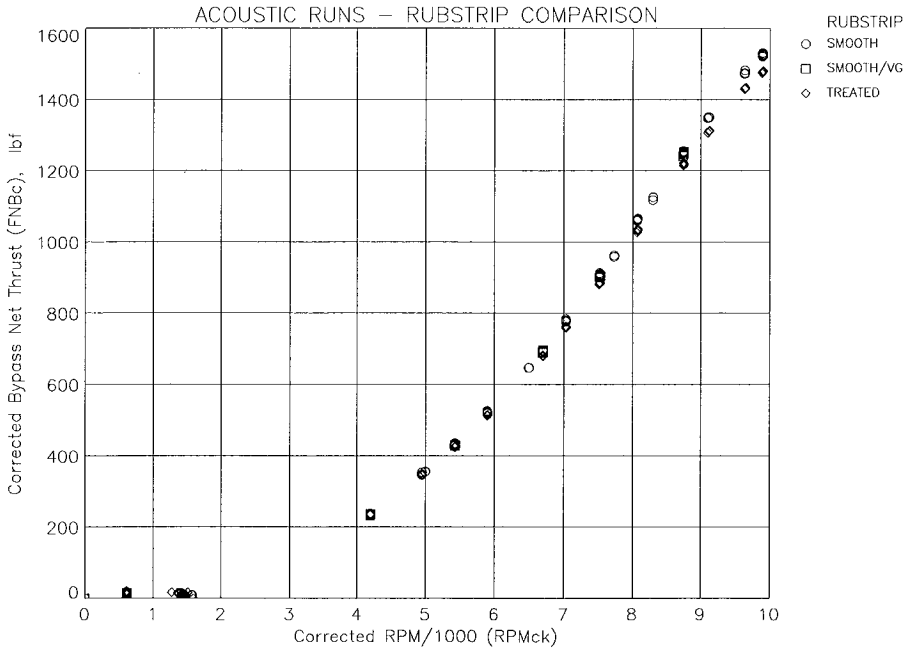

Figure 19. Bypass Corrected Net Thrust vs RPMc/1000, with Two Rubstrips, on Operating Line, Aeroacoustically Clean

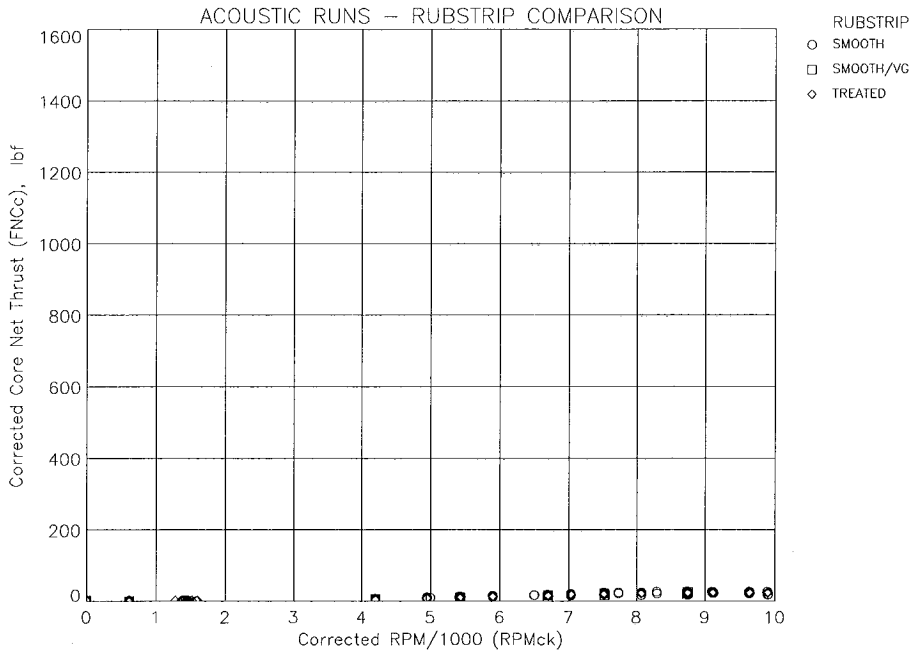

Figure 20. Core Corrected Net Thrust vs RPMc/1000, with Two Rubstrips, on Operating Line, Aeroacoustically Clean

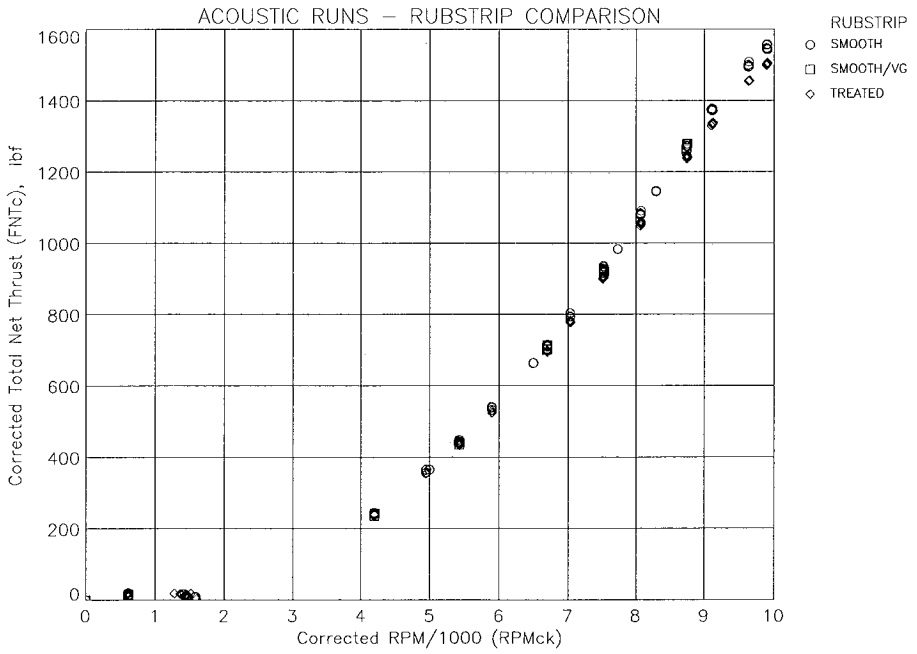

Figure 21. Total Corrected Net Thrust vs RPMc/1000, with Two Rubstrips, on Operating Line, Aeroacoustically Clean

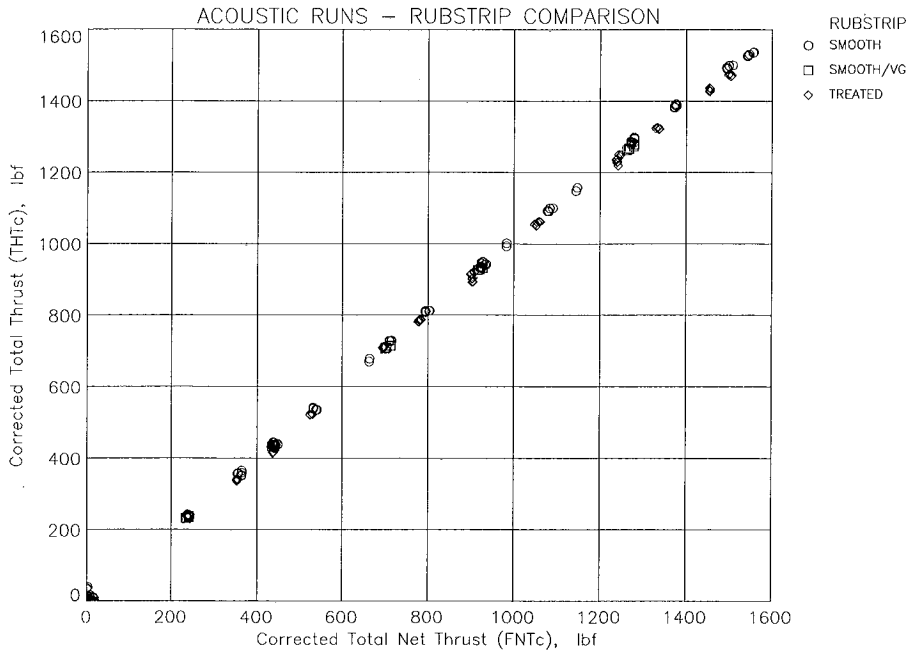

Figure 22. Balance Total Corrected Thrust vs Total Corrected Net Thrust with Two Rubstrips, on Operating Line, Aeroacoustically Clean

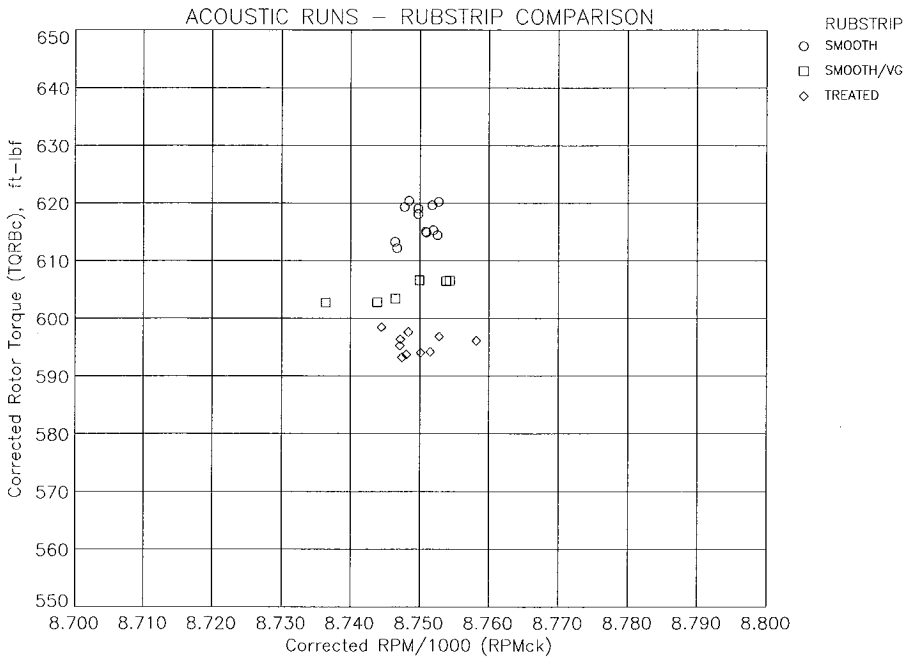

Figure 23. Rotor Balance Corrected Torque vs RPMc/1000, with Two Rubstrips, Near Takeoff, Aeroacoustically Clean

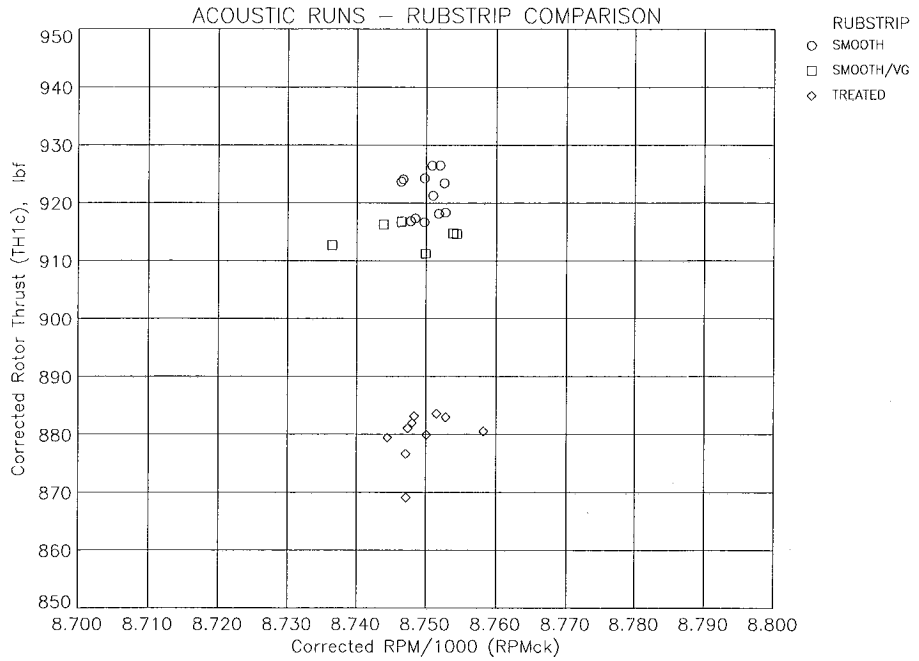

Figure 24. Rotor Balance Corrected Thrust vs RPMc/1000, with Two Rubstrips, Near Takeoff, Aeroacoustically Clean

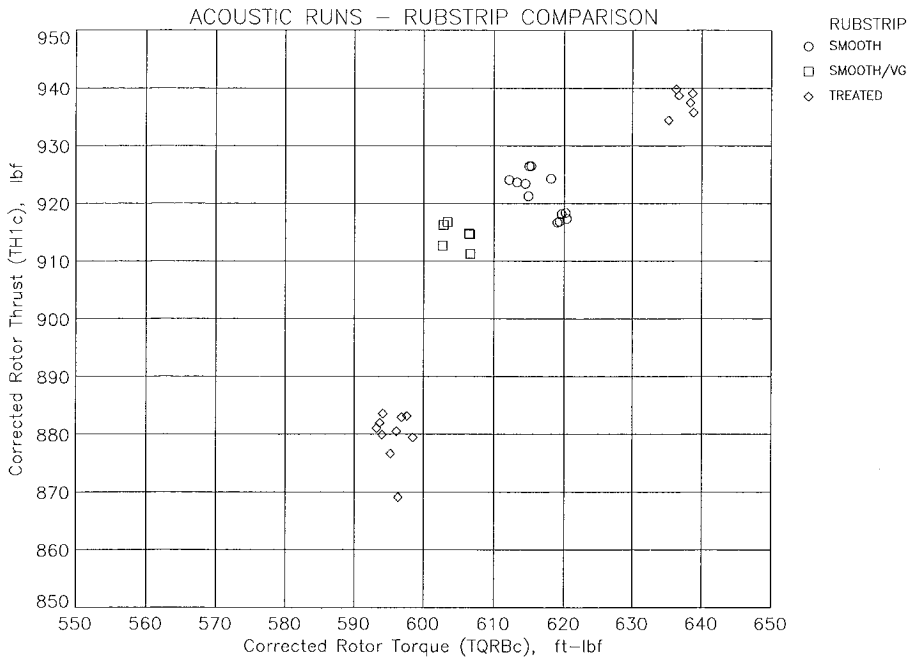

Figure 25. Rotor Balance Corrected Thrust vs Rotor Balance Corrected Torque, with Two Rubstrips, Near Takeoff, Aeroacoustically Clean

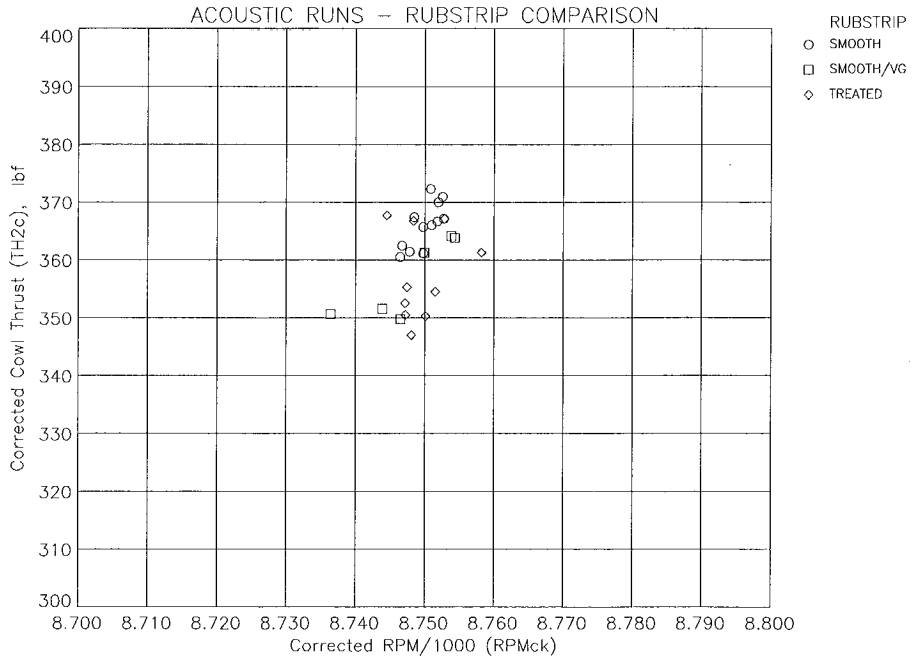

Figure 26. Cowl Balance Corrected Thrust vs RPMc/1000, with Two Rubstrips, Near Takeoff, Aeroacoustically Clean

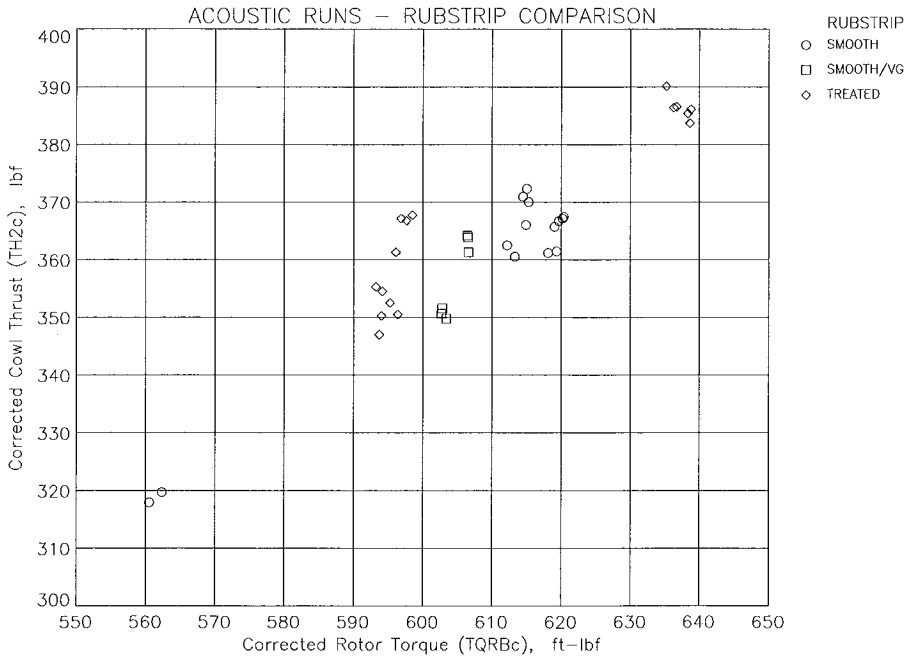

Figure 27. Cowl Balance Corrected Thrust vs Rotor Balance Corrected Torque, with Two Rubstrips, Near Takeoff, Aeroacoustically Clean

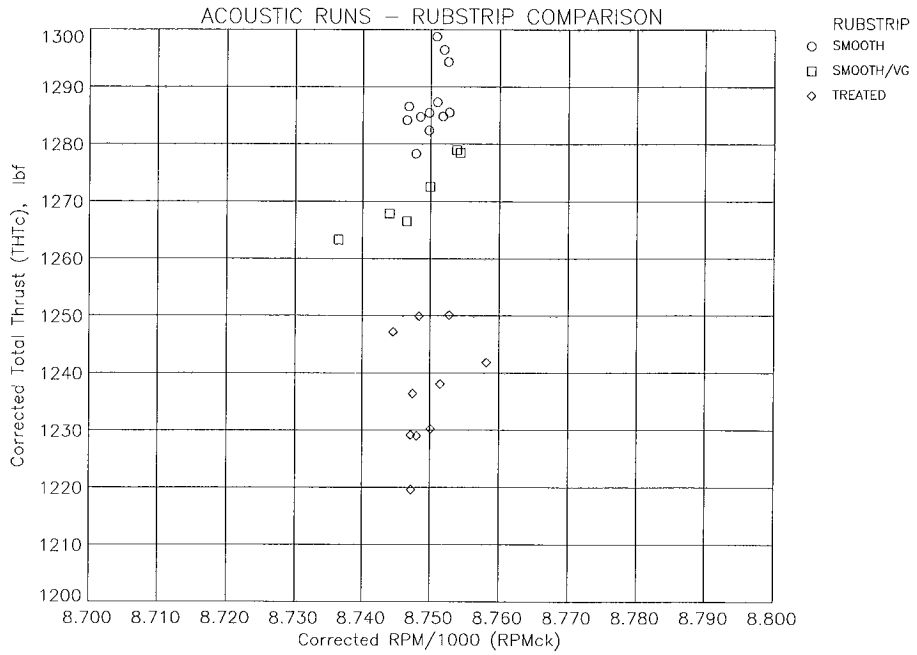

Figure 28. Total Corrected Thrust vs RPMc/1000, with Two Rubstrips, Near Takeoff, Aeroacoustically Clean

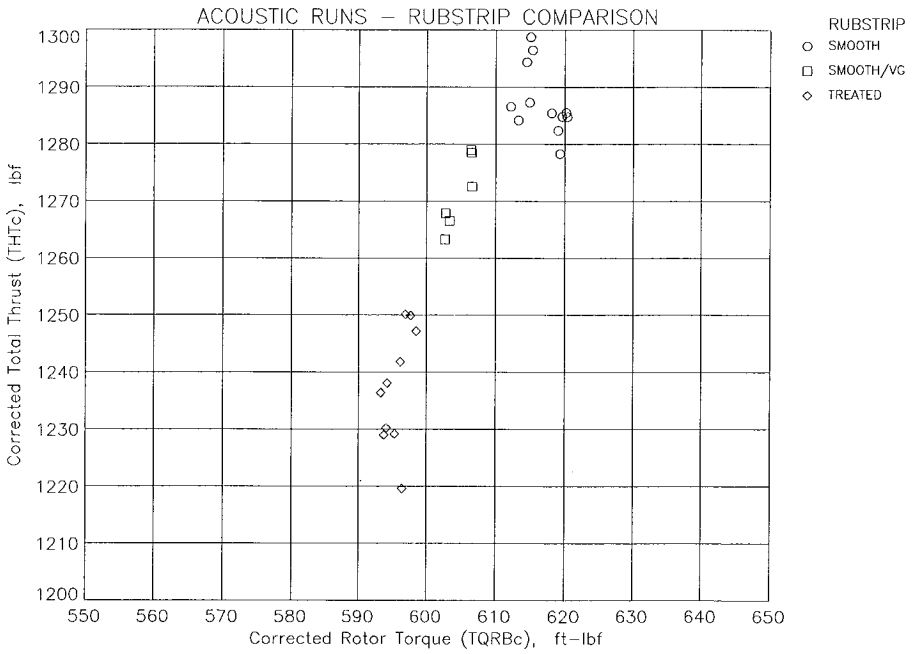

Figure 29. Cowl Balance Corrected Thrust vs Rotor Balance Corrected Torque, with Two Rubstrips, Near Takeoff, Aeroacoustically Clean

REPORT DOCUMENTATION PAGE

Form Approved
OMB No. 0704-0188

1. AGENCY USE ONLY (*Leave blank*)	2. REPORT DATE	3. REPORT TYPE AND DATES COVERED
	July 1998	Technical Memorandum

4. TITLE AND SUBTITLE

Model Engine Performance Measurement From Force Balance Instrumentation

5. FUNDING NUMBERS

WU–538–03–11–00

6. AUTHOR(S)

Robert J. Jeracki

7. PERFORMING ORGANIZATION NAME(S) AND ADDRESS(ES)

National Aeronautics and Space Administration
Lewis Research Center
Cleveland, Ohio 44135–3191

8. PERFORMING ORGANIZATION REPORT NUMBER

E–11263

9. SPONSORING/MONITORING AGENCY NAME(S) AND ADDRESS(ES)

National Aeronautics and Space Administration
Washington, DC 20546–0001

10. SPONSORING/MONITORING AGENCY REPORT NUMBER

NASA TM—1998-208486
AIAA–98–3112

11. SUPPLEMENTARY NOTES

Prepared for the 34th Joint Propulsion Conference cosponsored by AIAA, ASME, SAE, and ASEE, Cleveland, Ohio, July 12–15, 1998. Responsible person, Robert J. Jeracki, organization code 5940, (216) 433–3917.

12a. DISTRIBUTION/AVAILABILITY STATEMENT

Unclassified - Unlimited
Subject Categories: 02 and 07 Distribution: Nonstandard

This publication is available from the NASA Center for AeroSpace Information, (301) 621–0390.

12b. DISTRIBUTION CODE

13. ABSTRACT ***(Maximum 200 words)***

A large scale model representative of a low-noise, high bypass ratio turbofan engine was tested for acoustics and performance in the NASA Lewis 9– by 15–Foot Low-Speed Wind Tunnel. This test was part of NASA's continuing Advanced Subsonic Technology Noise Reduction Program. The low tip speed fan, nacelle, and an un-powered core passage (with core inlet guide vanes) were simulated. The fan blades and hub are mounted on a rotating thrust and torque balance. The nacelle, bypass duct stators, and core passage are attached to a six component force balance. The two balance forces, when corrected for internal pressure tares, measure the total thrust-minus-drag of the engine simulator. Corrected for scaling and other effects, it is basically the same force that the engine supports would feel, operating at similar conditions. A control volume is shown and discussed, identifying the various force components of the engine simulator thrust and definitions of net thrust. Several wind tunnel runs with nearly the same hardware installed are compared, to identify the repeatability of the measured thrust-minus-drag. Other wind tunnel runs, with hardware changes that affected fan performance, are compared to the baseline configuration, and the thrust and torque effects are shown. Finally, a thrust comparison between the force balance and nozzle gross thrust methods is shown, and both yield very similar results.

14. SUBJECT TERMS

Ducted fans; Thrust; Performance; Turbofan; Simulator

15. NUMBER OF PAGES

32

16. PRICE CODE

A03

17. SECURITY CLASSIFICATION OF REPORT	18. SECURITY CLASSIFICATION OF THIS PAGE	19. SECURITY CLASSIFICATION OF ABSTRACT	20. LIMITATION OF ABSTRACT
Unclassified	Unclassified	Unclassified	